Improved Model Predictive Control of Permanent Magnet Synchronous Motor with Duty Ratio Optimization and Cost Function Correction

Ming Liu, Jiefeng Hu, Senior Member, IEEE and K.W. Chan, Member, IEEE
Department of Electrical Engineering, The Hong Kong Polytechnic University, Hong Kong
Email: leo.m.liu@connect.polyu.hk

Abstract--**This paper presents an improved model predictive control (MPC) for permanent magnet synchronous motor (PMSM) drives. The proposed MPC is different from the conventional MPC in applying two voltage vectors in every control period. The duty ratio is firstly calculated using a simple but effective method with the consideration of the one-step delay. The cost function is then modified by incorporating the duty ratio, thus to calculate the optimal voltage vector applied in every sampling period. Test results show that the proposed control strategy contributes to lower torque and flux ripples compared to the existing MPC.**

Index Terms—**Cost function correction, duty ratio optimization, model predictive control (MPC), Permanent magnet synchronous motor (PMSM).**

I. Introduction

Direct torque control (DTC) and model predictive torque control (MPC) are two prevalent control strategies for permanent magnet synchronous motor (PMSM) drives. Conventional switching table based DTC has the advantages including simple structure, fast dynamic response and straight-forward algorithm, while it suffers unsatisfactory high torque and flux ripples. These ripples are reduced effectively with the compensation of the one step delay (OSD) [1] and duty ratio calculation[2].

In recent years, various model predictive control (MPC) have continually been proposed to control the power converters in different application areas, such as power grid [3, 4] and PMSM [5-7]. Different from DTC that voltage vectors are predefined in a switching table, MPTC directly chooses the optimal voltage vector by a cost function with quantified torque and flux ripples.

By introducing a zero vector in a sampling period, the torque and flux ripples can be further reduced [8]. In these approaches, the active vector is first selected from the cost function, then the duty ratio is determined based on a certain principle such as deadbeat control [5]. The active voltage vector selected in this way, however, may be no longer the optimal one when a null voltage vector is inserted along with it. In this paper, to tackle the aforementioned problem, the duty ratio is firstly calculated by a simplified but effective method with the consideration of the one-step delay. Then, the modified cost function integrated with the duty ratio is used obtain the optimal voltage vectors.

II. Mathematical Model

The mathematical model of PMSM can be developed in either the dq synchronous coordinate or the αβ stationary coordinate. For the d-q synchronous coordinate, all values of stator currents (i_d and i_q) and voltages (u_d and u_q) are constant. Assuming the back electromagnetic force is sinusoidal, and the magnetic hysteresis and eddy current losses are neglectable, the mathematical model of a PMSM in the dq synchronous coordinate is

$$u_s = R_s i_s + \frac{d\varphi_s}{dt} + j\omega\varphi_s \tag{1}$$

$$\varphi_s = L_d i_d + \varphi_f + jL_q i_q \tag{2}$$

$$T_e = \frac{3}{2}p(\varphi_s \times i_s) \tag{3}$$

More specifically, the mathematical model can be rewritten as

$$u_d = R_s i_d + \frac{d\varphi_d}{dt} - \omega\varphi_q \tag{4}$$

$$u_q = R_s i_q + \frac{d\varphi_q}{dt} + \omega\varphi_d \tag{5}$$

$$\varphi_d = L_d i_d + \varphi_f \tag{6}$$

$$\varphi_q = L_q i_q \tag{7}$$

$$T_e = \frac{3}{2}N(\varphi_d i_q - \varphi_q i_d) \tag{8}$$

where

R_s stator resistance
ω rotor speed
φ_f permanent magnet flux
N number of pole pairs
L_s, L_d, L_q stator inductance vector, d-axis inductance component and q-axis inductance component
i_s, i_d, i_q stator current vector, d-axis current component and q-axis current component
u_s, u_d, u_q stator voltage vector, d-axis voltage component and q-axis voltage component
$\varphi_s, \varphi_d, \varphi_q$ stator flux vector, d-axis flux component and q-axis flux component
T_e electromagnetic torque

Combining (4)-(7), the dq current equations can be expressed as

$$\frac{di_d}{dt} = \frac{-R_s i_d + \omega L_q i_q + u_d}{L_d} \tag{9}$$

$$\frac{di_q}{dt} = \frac{-R_s i_q - \omega L_d i_d + u_q + \varphi_f}{L_d} \tag{10}$$

The mechanical equation is introduced to be

$$T_e - T_L = J\frac{d\omega}{dt} + f\omega \tag{11}$$

where J is the rotational inertia, f is the viscous friction coefficient.

The speed differentiation with respect to time is

$$\frac{d\omega}{dt} = \frac{T_e - T_L - f\omega}{J} \tag{12}$$

III. PRINCIPLE OF PROPOSED MPC

The null voltage vector (V_0 or V_7) can decrease the torque, while nonzero voltage vector ($V_1, \dots V_6$) can increase the torque. With the usage both null voltage vector and nonzero voltage vector in one sampling period, the torque and flux ripple can be theoretically reduced. The essential problem is the method to calculate the optimal action duration of both the null and nonzero voltage vector. In other words, it is to find the duty ratio of the nonzero voltage vector. Three different methods are listed to calculated the duty ratio [5]. However, these methods are complicated and parameter dependent, and the duty ratio is calculated and implemented after obtaining the optimal voltage vector. The chosen active voltage vector without the consideration of duty ratio, however, may be no longer the optimal one.

In this paper, to tackle the aforementioned problem, first of all, a simple but effective method is implemented with the consideration of the one-step delay in this paper [2]. Then, the modified cost function integrated with the duty ratio is used to obtain the optimal voltage vectors. Besides, two methods for further improvement are proposed to reduce torque and flux ripples.

A. Duty Ratio Optimization

Since the torque and stator flux are the controlled variables, actual torque and flux are measured first for the MPC controller. After obtaining the measured current at kth sampling instant, the torque and flux are calculated as

$$\varphi_s{}^k = L_d i_d{}^k + \varphi_f + jL_q i_q{}^k \quad (13)$$

$$T_e{}^k = \frac{3}{2}p(\varphi_d{}^k i_q{}^k - \varphi_q{}^k i_d{}^k) \quad (14)$$

Once the measured torque and flux are obtained, they are used together with the references to calculate the duty ratio. To avoid the complicated calculation, a simple but effective method is adopted [2]. The duty ratio d^k at the kth sampling instant is

$$\mathrm{d}^k = \left|\frac{T_e{}^k - T^*}{U_T}\right| + \left|\frac{\varphi_s{}^k - \varphi^*}{U_\varphi}\right| \quad (15)$$

where T^* and φ^* are the reference torque and flux. U_T and U_φ are the user defined positive constant (for example, $U_T = 2$, $U_\varphi = 0.2$). Usually, larger values of U_T and U_φ result in lower torque and flux ripples, but the dynamic response degraded.

The d-q currents at $(k+1)th$ sampling instant are derived based on (9) and (10).

$$i_d{}^{k+1} = i_d{}^k + \frac{\mathrm{d}^k T_s}{L_d}\left(-R_s i_d{}^k + \omega^k L_q i_q{}^k + u_d{}^k\right) + \frac{(1-\mathrm{d}^k)T_s}{L_d}\left(-R_s i_d{}^k + \omega^k L_q i_q{}^k\right) \quad (16)$$

$$i_q{}^{k+1} = i_q{}^k + \frac{\mathrm{d}^k T_s}{L_q}\left(-R_s i_q{}^k - \omega^k L_d i_d{}^k + u_q{}^k - \omega^k \varphi_f\right) + \frac{(1-\mathrm{d}^k)T_s}{L_d}\left(-R_s i_q{}^k - \omega^k L_d i_d{}^k - \omega^k \varphi_f\right) \quad (17)$$

where T_s is the sampling time. ω^k is the measured speed at kth sampling instant.

Then, the flux and torque at $(k+1)th$ sampling instant can be derived as (19) and (20)

$$\varphi_s{}^{k+1} = L_d i_d{}^{k+1} + \varphi_f + jL_q i_q{}^{k+1} \quad (18)$$

$$T_e{}^{k+1} = \frac{3}{2}p(\varphi_s{}^{k+1} \times i_s{}^{k+1}) \quad (19)$$

Considering the one-step delay compensation, the torque in k+2 sampling instant period should be used to develop the cost function.

The duty ratio at the $(\mathrm{k}+1)$th sampling instant is

$$\mathrm{d}^{k+1} = \left|\frac{T^{k+1} - T^*}{U_T}\right| + \left|\frac{\varphi^{k+1} - \varphi^*}{U_\varphi}\right| \quad (20)$$

Repeating the previous steps, the d-q currents at $(k+2)th$ sampling instant are derived accordingly.

$$i_d{}^{k+2} = i_d{}^{k+1} + \frac{\mathrm{d}^{k+1} T_s}{L_d}(-R_s i_d{}^{k+1} + \omega^{k+1} L_q i_q{}^{k+1} + u_d{}^{k+1}) + \frac{(1-\mathrm{d}^{k+1})T_s}{L_d}(-R_s i_d{}^{k+1} + \omega^{k+1} L_q i_q{}^{k+1}) \quad (21)$$

$$i_q{}^{k+2} = i_q{}^{k+1} + \frac{\mathrm{d}^{k+1} T_s}{L_q}(-R_s i_q{}^{k+1} - \omega^{k+1} L_d i_d{}^{k+1} + u_q{}^{k+1} - \omega^k \varphi_f) + \frac{(1-\mathrm{d}^{k+1})T_s}{L_d}(-R_s i_q{}^{k+1} - \omega^k L_d i_d{}^{k+1} - \omega^{k+1} \varphi_f) \quad (22)$$

Consequently, the flux and torque at $(k+2)th$ sampling instant can be derived as (23) and (24)

$$\varphi_s{}^{k+2} = L_d i_d{}^{k+2} + \varphi_f + jL_q i_q{}^{k+2} \quad (23)$$

$$T_e{}^{k+2} = \frac{3}{2}p(\varphi_s{}^{k+2} \times i_s{}^{k+2}) \quad (24)$$

In (23) and (24), only $u_s{}^{k+1}$, i.e., $u_d{}^{k+1}$ and $u_q{}^{k+1}$, is the unknown variable. Using (23) and (24) to develop the cost function

$$min.\, g = \left|T_e{}^{k+2} - T^*\right| + k1\left|\varphi_s{}^{k+2} - \varphi^*\right| \quad (25)$$
$$\mathrm{s.t.}\, u_s{}^{k+1} \in \{V_0, V_1, \dots V_6, V_7\}$$

where $k1$ is the weighting factor, which is defined as the ratio of reference torque and permanent magnet flux, i.e. $k1 = \frac{T^*}{\varphi^*}$.

Eight voltage vectors are evaluated to obtain the optimal one, and the duty ratio at the $(k+1)th$ sampling instant d^{k+1} will be used along with the selected optimal voltage vector. It is noted that the null vectors (either V_0 (000) or V_7 (111)) should be chosen properly to reduce the switching frequency.

B. k1 Elimination

For the cost function in (25), there is a weighting factor k1 for adjusting the priority of torque and flux ripple minimization, which is still an open question. A new method to define eliminate k1 is proposed here. The cost function is improved to be

$$min.\, g = \left|\frac{T_e{}^{k+2} - T^*}{T^*}\right| + \left|\frac{\varphi_s{}^{k+2} - \varphi^*}{\varphi^*}\right| \quad (26)$$
$$\mathrm{s.t.}\, u_s{}^{k+1} \in \{V_0, V_1, \dots V_6, V_7\}$$

The new cost function has different physical meaning from (25). $\left|\frac{T_e{}^{k+2} - T^*}{T^*}\right|$ indicates the percentage error between the predictive torque $T_e{}^{k+2}$ and reference torque T^*. Similarly, $\left|\frac{\varphi_s{}^{k+2} - \varphi^*}{\varphi^*}\right|$ indicates the percentage error between the predictive stator flux $\varphi_s{}^{k+2}$ and reference torque φ^*. This method is simple and effective to develop the cost function, and torque and flux ripples can be reduced to some extent.

C. Stability Factor

For the cost function shown in paper [7], two additional items are added:

$$min.\, g = \left|T_e{}^{k+2} - T^*\right| + \left|\varphi_s{}^{k+2} - \varphi^*\right| + \mathrm{A}\left(\left|T_e{}^{k+N} - T^*\right| + k1\left|\varphi_s{}^{k+N} - \varphi^*\right|\right)$$

$$+\mathrm{B}\left(\sum_{i=a,b,c}\left|u_s^{k+1}(S_i)-u_s^k(S_i)\right|\right)$$
$$\mathrm{s.t.}\,{u_s}^{k+1}\in\{V_0,V_1,\ldots V_6,V_7\} \qquad (27)$$

The third term is to reducing switching frequency, which will not be included in this paper. The second term is introduced to consider the errors in the *(k+N)th* sampling instant with the weighting factor A. Considering the elimination of k1 and taking advantage of the second term, the cost function can be redeveloped to be

$$min.\,g=\left|\frac{{T_e}^{k+2}-T^*}{T^*}\right|+\left|\frac{{\varphi_s}^{k+2}-\varphi^*}{\varphi^*}\right|$$
$$+\frac{1}{3}\left(\left|\frac{{T_e}^{k+3}-T^*}{T^*}\right|+\left|\frac{{\varphi_s}^{k+3}-\varphi^*}{\varphi^*}\right|\right)$$
$$+\frac{1}{5}\left(\left|\frac{{T_e}^{k+5}-T^*}{T^*}\right|+\left|\frac{{\varphi_s}^{k+5}-\varphi^*}{\varphi^*}\right|\right)$$
$$\mathrm{s.t.}\,{u_s}^{k+1}\in\{V_0,V_1,\ldots V_6,V_7\} \qquad (28)$$

where

$${T_e}^{k+i}={T_e}^{k+1}+(\mathrm{i}-1)({T_e}^{k+2}-{T_e}^{k+1})$$
$${\varphi_s}^{k+i}={\varphi_s}^{k+1}+(\mathrm{i}-1)({\varphi_s}^{k+2}-{\varphi_s}^{k+1})$$

The weighting factor of $(k+i)th$ parameters is defined as $\frac{1}{i}$. It is reasonable that the predictive accuracy deteriorates with the incearse of i. The diagram of the proposed MPC is shown in Fig. 1.

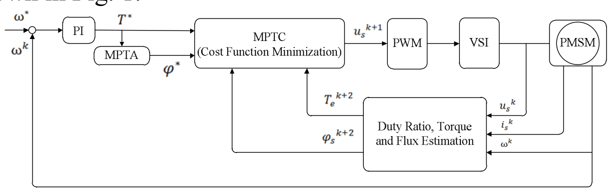

Fig. 1. Block diagram of the proposed MPC

IV. SIMULATION RESULTS

In order to compare the proposed MPC with different control strategies, 6 different simulations have been carried out:

1. DTC with OSD compensation (one voltage vector in a sampling period).
2. MPC with OSD compensation (one voltage vector in a sampling period).
3. MPC with duty ratio (two voltage vectors in a sampling period, while the duty ratio is calculated in the last step).
4. MPC with duty ratio optimization (in section III. A)
5. MPC with k1 elimination (in section III. B)
6. MPC with stability factor (in section III. C)

The simulation parameters of PMSM and control system are tabulated in Table I.

Table I. Simulation parameters

Number of pole pairs	N	3
Permanent magnet flux	φ_f	0.21134 Wb
Stator resistance	R_s	1.132 Ω
d- and q-axis inductance	L_d, L_q	12.38 mH, 15.72 mH
Reference speed	n	500 rpm
Load torque	T_L	2 Nm
DC bus voltage	U_N	310 V
Sampling frequency	f_s	10 kHz
Sampling time	T_s	100 us

A. Steady Response

The steady response is tested in this section. Two typical simulation results are shown in Fig. 1, i.e., MPC with duty ratio and MPC with stability factor. Red and blue curves are reference and simulation values. From top to bottom, the curves are speed, torque, stator flux and stator current in phase A. By comparing the simulation results, it is seen that the proposed MPC with stability factor has lower torque and flux ripples. Besides, the waveform quality is improved by using the proposed MPC with stability factor. After comparing the simulation results of 6 control strategies, the proposed MPC with stability factor shows the best performance in terms of torque ripple, flux ripple and stator current waveform quality at 500 rpm.

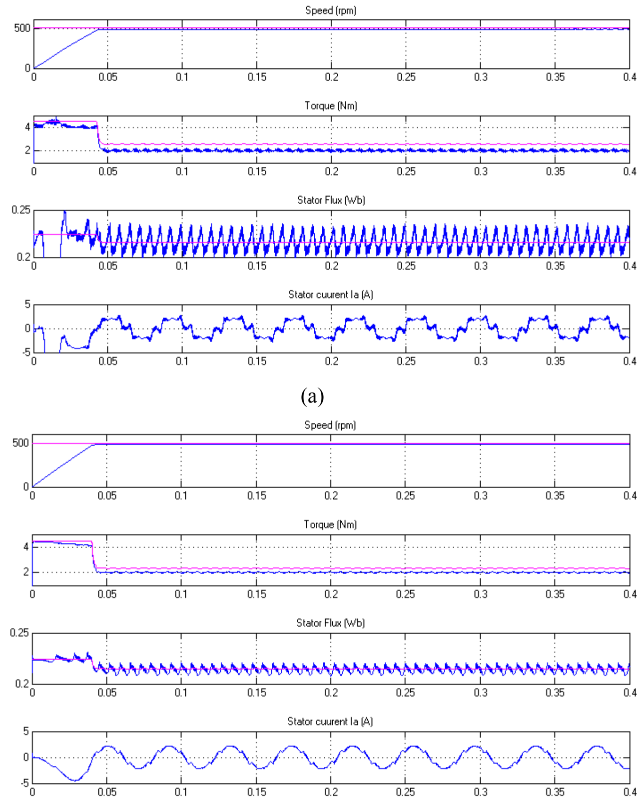

(b)

Fig. 2. Steady response at 500 rpm with 2 Nm load (a) MPTC with duty ratio (b) MPC with stability factor

B. Dynamic Response

In order to test start-up response and dynamic response, simulation results with different speed (500 rpm, 1000 rpm and 1500 rpm) were carried out as shown in Fig. 3. All simulation parameters are the same for 6 control strategies as is shown in Table I. The simulation results show that the performance of different control strategies may change with different speed.

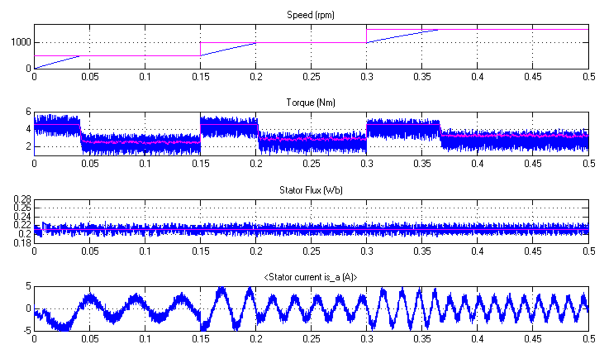

(a)

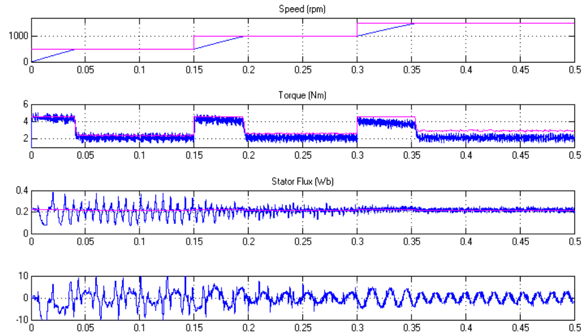

(b)

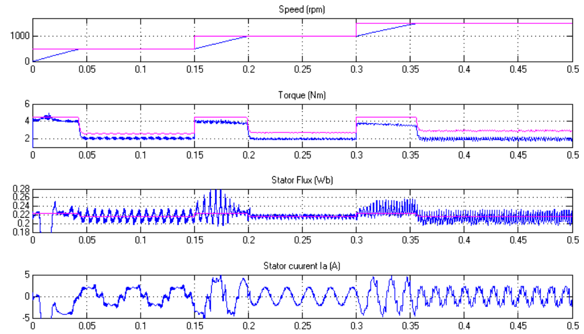

(c)

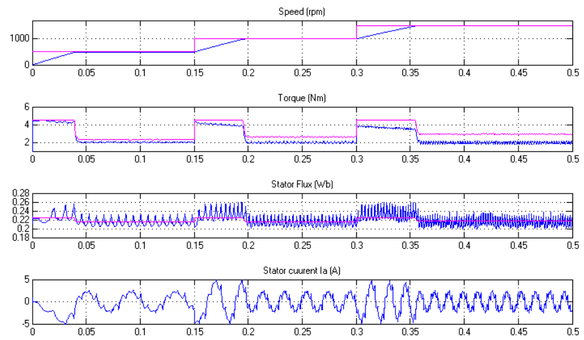

(d)

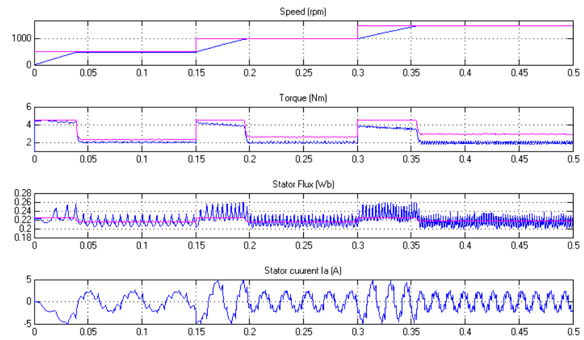

(e)

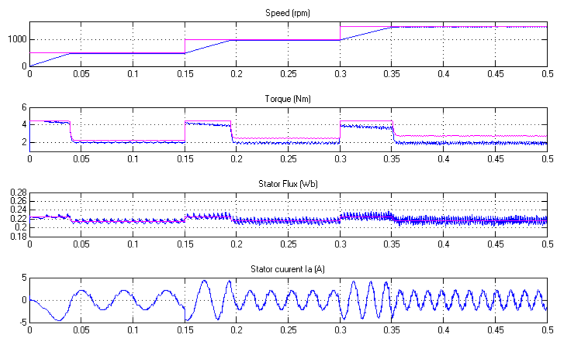

(f)

Fig.3. Dynamic response with 2N load (a) DTC with OSD compensation (b) MPC with OSD compensation (c) MPC with duty ratio (d) MPC with duty ratio optimization (e) MPC with k1 elimination (f) MPC with stability factor

Flux and torque ripples are quantified using the standard deviation based on the collected data during the period from 0.1 s to 0.11 s (500 rpm), 0.25 s to 0.26 s (1000 rpm) and 0.4 s to 0.41 s (1500 rpm).

$$\varphi_{rip} = \sqrt{\frac{1}{N}\sum_{i=1}^{N}(\varphi_s(i) - \varphi_{av})^2} \quad (29)$$

$$T_{rip} = \sqrt{\frac{1}{N}\sum_{i=1}^{N}(T_e(i) - T_{av})^2} \quad (30)$$

The quantitative results of different control strategies are summarized in Table II.

Method	φ_{rip} (Wb)	T_{rip} (Nm)
DTC with OSD compensation	0.0074	0.6159
MPC with OSD compensation	0.0541	0.2379
MPC with duty ratio	0.0087	0.07
MPC with duty ratio optimization	0.0072	0.0436
MPC with k1 elimination	0.0067	0.0412
MPC with stability factor	0.0026	0.0298

(a)

Method	φ_{rip} (Wb)	T_{rip} (Nm)
DTC with OSD compensation	0.0074	0.6057
MPC with OSD compensation	0.023	0.237
MPC with duty ratio	0.0027	0.0529
MPC with duty ratio optimization	0.0074	0.0781
MPC with k1 elimination	0.0058	0.0776
MPC with stability factor	0.0046	0.0705

(b)

Method	φ_{rip} (Wb)	T_{rip} (Nm)
DTC with OSD compensation	0.0073	0.6279
MPC with OSD compensation	0.0121	0.2164
MPC with duty ratio	0.0089	0.1346
MPC with duty ratio optimization	0.0083	0.1188
MPC with k1 elimination	0.0068	0.114
MPC with stability factor	0.0054	0.0952

(c)

Table II. Comparison of different control schemes in terms of flux and torque ripples in different speed (a) 500 rpm (b) 1000 rpm (c) 1500 rpm

To achieve the intuitive comparison, the bar graph is depicted as shown in Fig. 4.

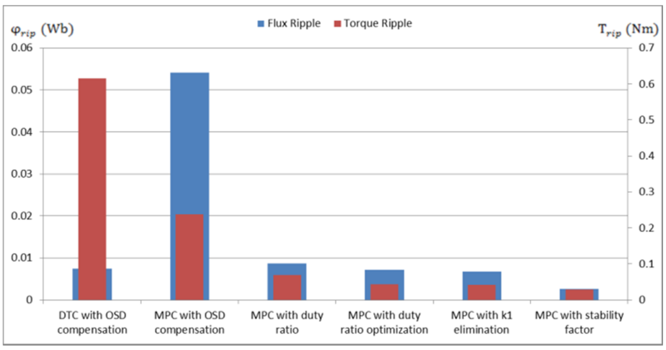

(a)

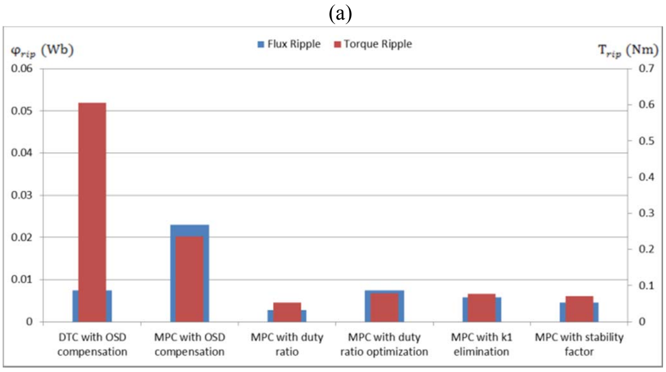

(b)

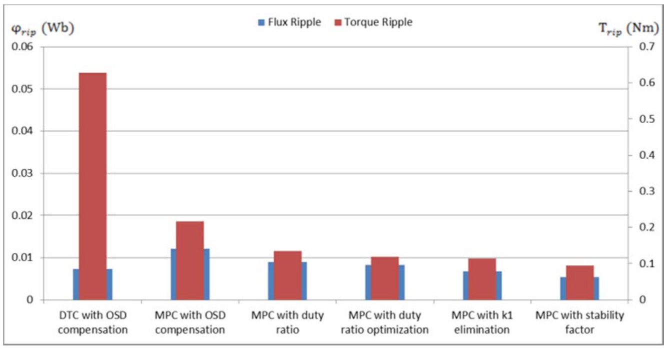

(c)

Fig. 4 Comparison of different control schemes in terms of flux and torque ripples in different speed (a) 500 rpm (b) 1000 rpm (c) 1500 rpm

From the Fig. 4, one can observe that 6 control strategies show various characteristics at different speed. For the control strategy of DTC with OSD compensation, varying speed will change the performance insignificantly in terms of torque and flux ripples. Specifically, torque and flux ripples are consistently about 0.61 Nm and 0.0074 Wb. The flux ripple is acceptable with respect to different speed, while the torque ripple is too high comparing to other control strategies.

With regard to the control strategy of MPC with OSD compensation, the torque ripple is almost constant for different speed. The flux ripple reduces gradually with the increase of speed. The reason could be that the cost function based MPC method is more accurate to select the voltage vector than the switching table based DTC method, since DTC only consider the positive and negative signs of torque and flux differences to determine the optimal voltage vector. However, these two control strategies are uncompetitive compared with the rest four control strategies.

For the proposed control strategies, it is seen that torque and flux ripples decreases gradually with the step-by-step improvement. The control strategy of MPC with stability factor is the best control strategy among three proposed control strategies in terms of torque and flux ripples. However, with the increase of speed, the value of torque ripple increases accordingly. Apart from the control method of MPC with k1 elimination, the flux ripple shows the same phenomenon.

For some specific speed range (around 1000 rpm), the MPC that the duty ratio is calculated in the last step shows the excellent performance. Nevertheless, the proposed MPC with stability factor presents a satisfying performance with respect to torque and flux ripples in a wide speed range.

In addition to ripples, the proposed MPC with stability factor demonstrates the fastest dynamic response among 6 control strategies. By using this control strategy, PMSM can reach the reference speed with the minimum time period. Moreover, it shows the best performance of the start-up response. The over shoot current is the minimum value among 6 simulations. Table III gives the best control strategy corresponding to different conditions.

Table III. Best control strategy corresponding to different speed (3 is MPC with duty ratio, while 6 is MPC with stability factor)

Speed (rpm)	500	1000	1500
Best control strategy in terms of φ_{rip}	6	3	6
Best control strategy in terms of T_{rip}	6	3	6
Smallest current total harmonic distortion	6	3	6
Fastest dynamic response	6	6	6
Best start-up response	6		

V. CONCLUSION

In this paper, an improved model predictive control is proposed with the optimization of duty ratio and the correction of cost function. Different from the previous MPC that the duty ratio is derived at the last step, the duty ratio is integrated into the cost function to derive optimal voltage vector. Besides, the MPC with the elimination of weighting factor k1 and the compensation of stability factor is firstly proposed to improve the cost function. The performance of the proposed control strategy is compared with other three existing control strategies using simulations. The proposed control strategy presents the merits of fastest dynamic response, best start-up response and lowest torque and flux ripple in a wide speed range.

VI. REFERENCES

[1] Y. Zhang, J. Zhu, and W. Xu, "Analysis of one step delay in direct torque control of permanent magnet synchronous motor and its remedies," in *2010 International Conference on Electrical Machines and Systems*, 2010, pp. 792-797.

[2] Y. Zhang and J. Zhu, "Direct Torque Control of Permanent Magnet Synchronous Motor With Reduced Torque Ripple and Commutation Frequency," *IEEE Transactions on Power Electronics,* vol. 26, pp. 235-248, 2011.

[3] J. Hu, J. Zhu, G. Lei, G. Platt, and D. G. Dorrell, "Multi-Objective Model-Predictive Control for High-Power Converters," *IEEE Transactions on Energy Conversion,* vol. 28, pp. 652-663, 2013.

[4] J. Hu and K. W. E. Cheng, "Predictive Control of Power Electronics Converters in Renewable Energy Systems," *Energies,* vol. 10, p. 515, 2017.

[5] Z. Yongchang and W. Xianglong, "Torque ripple RMS minimization in model predictive torque control of PMSM drives," in *2013 International Conference on Electrical Machines and Systems (ICEMS)*, 2013, pp. 2183-2188.

[6] H. Zhu, X. Xiao, and Y. Li, "Torque Ripple Reduction of the Torque Predictive Control Scheme for Permanent-Magnet Synchronous Motors," *IEEE Transactions on Industrial Electronics,* vol. 59, pp. 871-877, 2012.

[7] Y. Zhang, J. Zhu, and W. Xu, "Predictive torque control of permanent magnet synchronous motor drive with reduced switching frequency," in *2010 International Conference on Electrical Machines and Systems*, 2010, pp. 798-803.

[8] T. Wang, J. Zhu, and Y. Zhang, "Model predictive torque control for PMSM with duty ratio optimization," in *2011 International Conference on Electrical Machines and Systems*, 2011, pp. 1-5.